ACS SENSORS

pubs.acs.org/acssensors

Article

Avian Influenza Virus Detection by Optimized Peptide Termination on a Boron-Doped Diamond Electrode

Teruhiko Matsubara,[⊥] Michiko Ujie,[⊥] Takashi Yamamoto, Yasuaki Einaga, Tomo Daidoji, Takaaki Nakaya, and Toshinori Sato*

Cite This: https://dx.doi.org/10.1021/acssensors.9b02126

Read Online

ACCESS | Metrics & More | Article Recommendations | Supporting Information

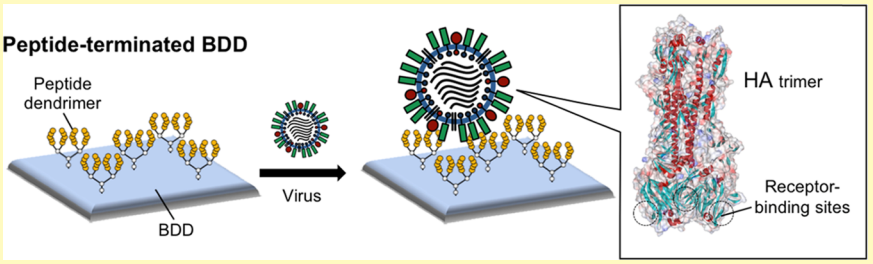

ABSTRACT: The development of a simple detection method with high sensitivity is essential for the diagnosis and surveillance of infectious diseases. Previously, we constructed a sensitive biosensor for the detection of pathological human influenza viruses using a boron-doped diamond electrode terminated with a sialyloligosaccharide receptor-mimic peptide that could bind to hemagglutinins involved in viral infection. Circulation of influenza induced by the avian virus in humans has become a major public health concern, and methods for the detection of avian viruses are urgently needed. Here, peptide density and dendrimer generation terminated on the electrode altered the efficiency of viral binding to the electrode surface, thus significantly enhancing charge-transfer resistance measured by electrochemical impedance spectroscopy. The peptide-terminated electrodes exhibited an excellent detection limit of less than one plaque-forming unit of seasonal H1N1 and H3N2 viruses. Furthermore, the improved electrode was detectable for avian viruses isolated from H5N3, H7N1, and H9N2, showing the potential for the detection of all subtypes of influenza A virus, including new subtypes. The peptide-based electrochemical architecture provided a promising approach to biosensors for ultrasensitive detection of pathogenic microorganisms.

KEYWORDS: *avian influenza virus, boron-doped diamond electrode, sialic acid-mimic peptide, electrochemical impedance spectroscopy, click chemistry, hemagglutinin, limit of detection*

Symptoms of influenza, such as fever, headache, and muscle pain, appear suddenly after a latent period of about 1−3 days but gradually disappear within 1 week.[1,2] However, high-risk groups, e.g., very young children, elderly individuals, and patients with underlying diseases, such as diabetes, may exhibit severe symptoms of infection; thus, treatment strategies, such as vaccination and/or anti-influenza drugs, are recommended.[3] Influenza diagnosis is often performed using patient specimens that contain viruses for anti-influenza therapy. However, these approaches require at least 1 day from the beginning of symptom onset to increase virus titers in the specimens because of the low limit of detection (LOD) (e.g., >1000 plaque-forming units [pfu]) of rapid diagnosis kits.[4,5] Rapid diagnosis kits are typically based on immunochromatography using antiviral nucleoprotein antibodies, and several types of colloidal particle-conjugated antibodies have been developed.[6] Recently, a fluorescence immunochromatography method with high sensitivity was developed using antihemagglutinin (HA) antibodies.[7] The sensitivity of this approach was reported to be at least 10-fold higher than that of the conventional system, although a dedicated fluorescence reader is required for detection.[8]

In recent decades, a novel boron-doped diamond (BDD)-based electrochemical sensor has been developed for the detection of inorganic ions, organic compounds, and biomolecules.[9−11] BDD is used as a working electrode, and the electrochemical characteristics, including a broad electrochemical potential range and a low background current, are superior to those of other conventional electrode materials, such as glassy carbon or platinum. In particular, the characteristic of weak molecule adsorption is advantageous for the development of specific biosensors because many types of biomolecules are found in biological samples. Some research groups have reported the detection of influenza virus (IFV)

Received: October 30, 2019
Accepted: January 30, 2020

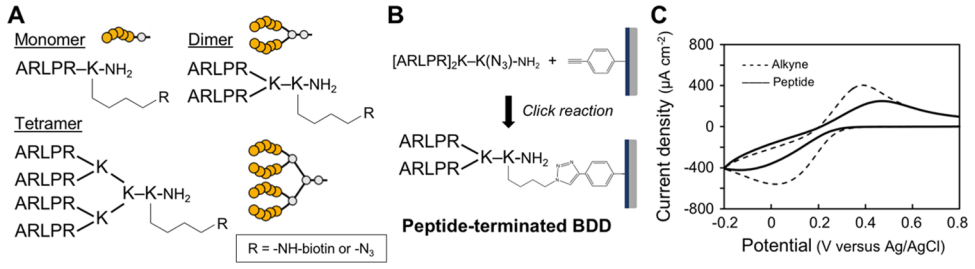

Figure 1. Preparation of the peptide-terminated BDD electrode. (A) Design of dendrimers having pentapeptide units that mimicked the sialylglycoconjugate receptor for IFV HA capture. The chemical structure of peptide dendrimers. First- (dimer) and second-generation (tetramer) dendrimers were branched with lysine (K) at the N^{α}- and N^{ε}-amino groups. The C-terminal lysine had a biotin or azide group as the side chain. (B) Peptide termination by the click reaction between the azide-conjugated peptide dimer ($[ARLPR]_2K\text{-}K(N_3)\text{-}NH_2$) and the alkyne-terminated BDD electrode. (C) CVs of 10 mM $K_3[Fe(CN)_6]$ using alkyne-terminated (dashed line) and peptide-terminated (solid line) BDD electrodes in 100 mM Na_2SO_4. The sweep rate was 100 mV/s.

using antibody-immobilized electrodes composed of gold,[12,13] silver/carbon,[14] and BDD.[15] Nidzworski et al. achieved the most sensitive IFV detection using an anti-M1 protein antibody-immobilized BDD electrode by electrochemical impedance spectroscopy (EIS) measurement, reporting a LOD of 1 fg/mL (5−10 viruses/sample).[15]

We have focused on the use of HA from IFV, which recognizes sialylglycoconjugate receptors on the cell surface at the initial step of infection.[2,16,17] Sialic acid-conjugated glycan has been applied for glycan microarray technology, and the determination of the receptor specificities of HA has been helpful for influenza research.[18,19] Recently, H1 and H5 HAs were detected on a sialyl lactose-immobilized field-effect transistor,[20,21] and IFV H3N2 was then detected.[22] However, the viral envelope also contains neuraminidase (NA), which can digest sialic acid (*N*-acetyl neuraminic acid) from the surface of host cells to release viral progeny;[3] therefore, the results of IFV detection using sialic acid-conjugated glycan may be underestimated. Actually, Zhang et al. measured the amount of glucose that is released from sialyl galactose by NA digestion to estimate the amount of IFV via a glucose sensor.[23]

The pentapeptide Ala-Arg-Leu-Pro-Arg rather than sialylglycoconjugates was designed to bind to the receptor-binding site of all types of HA.[24] Indeed, this pentapeptide binds to H1 and H3 HAs,[25] and the corresponding *N*-stearoyl derivatives and carbosilane-based dendrimers have inhibitory activity against both seasonal H1N1 and H3N2 IFV infections.[24,26] Peptides are easy to design and inexpensive to prepare; in practice, peptides can be produced for utilization as antigens[27] and drugs.[28] Moreover, in a previous study, this pentapeptide was immobilized on the BDD surface, and human IFVs were successfully detected by EIS measurements.[29] Compared with nonspecific adsorption of IFVs onto a peptide-immobilized glassy carbon electrode, the peptide-immobilized BDD electrode showed excellent detection of IFVs in the range of 20−400 pfu.

In the present study, we developed an improved sensor to enhance sensitivity and demonstrate the detection of avian IFVs. Divalent and tetravalent peptide dendrimers were immobilized, and the density of the dendrimer terminated on the BDD surface was then optimized for effective IFV detection. The electrode with the optimized density determined using a ferrocene-derivative dendrimer was found to enable ultrasensitive detection of seasonal H1N1 and H3N2 IFVs with an LOD of 0.33−0.91 pfu, indicating an order of magnitude better detection than that of the previous electrode. The tetravalent peptide dendrimer-immobilized BDD electrode showed the detection of avian IFVs of H5N3, H7N1, and H9N2 substrains. Thus, our results showed that this peptide-based electrode might have potential applications in the ultrasensitive detection of pathogens as well as glycan- and antibody-based sensors.

EXPERIMENTAL SECTION

HA and IFV. HAs, prepared from A/New Caledonia/20/99 (H1N1) and A/New York/55/2004 (H3N2) viruses, were kindly provided by Dr. Yujiro Suzuki (Kitasato Institute, Japan).[30]

Human IFVs, A/Puerto Rico/8/34 (H1N1) and A/Aichi/2/68 (H3N2), grown in allantoic cavity of embryonated chicken eggs, were obtained as described previously.[24] Avian IFVs isolated from embryonated chicken eggs, H5N3 (A/duck/Hong Kong/820/1980), H7N1 (A/duck/Hong Kong/301/1978), and H9N2 (A/duck/Hong Kong/448/1978),[31] were propagated according to a general protocol recommended by the World Health Organization for the isolation of influenza viruses in cell culture. Briefly, IFVs were used to infect a monolayer of Madin−Darby canine kidney (MDCK) cells and grown in 5 mL of Dulbecco's modified Eagle's medium until the cytopathic effect was observed (typically within a week). The medium was collected and centrifugated at 1680*g* (3000 rpm) for 5 min. The supernatant containing IFV was aliquoted and stored at −80 °C until use. The virus titers were determined by plaque assays,[32] and IFVs showed titers of approximately 300 pfu/μL in the supernatant. The amount of total protein in IFV stock was determined using bicinchoninic acid (Pierce BCA protein assay kit).

Peptide Dendrimers. The biotinyl peptide dimer (Ala-Arg-Leu-Pro-Arg)$_2$Lys-Lys(biotin) and the biotinyl peptide tetramer ([Ala-Arg-Leu-Pro-Arg]$_2$Lys)$_2$Lys-Lys(biotin) were obtained as described previously.[25]

The peptide dimer (Ala-Arg-Leu-Pro-Arg)$_2$Lys-Lys(N_3) and the ferrocenyl peptide dimer (ferrocene-Ala-Arg-Leu-Pro-Arg)$_2$Lys-Lys-(N_3) were obtained as described previously.[29] The peptide tetramer [(Ala-Arg-Leu-Pro-Arg)$_2$Lys]$_2$Lys-Lys(N_3) was obtained as a white powder (5.7 mg, 19%): matrix-assisted laser desorption ionization time-of-flight mass spectrometry (*m*/*z*: calculated molecular weight for $C_{128}H_{237}N_{55}O_{24}$ $[M+H]^+$ 2929.9; found 2932.3; Figure S1).

Electrochemistry. Electrochemical measurements were carried out with a standard three-electrode configuration using a potentiostat (CompactStat; Ivium Technologies, Eindhoven, the Netherlands). The BDD electrodes used as the working electrode were assembled as the bottom of a single-compartment cell with an O-ring (1.8 mm or 2.08 cm diameter). A Ag/AgCl (saturated KCl) electrode and a Pt wire electrode were used as the reference (+0.199 V versus standard hydrogen) and counter electrodes, respectively.

Click Reaction for Peptide Immobilization. The alkyne-terminated BDD substrate was prepared as described previously (Figure S2).[29,33,34]

Typically, the alkyne-terminated area was further incubated for 24 h in a solution (6 mL) of 1−26 μM peptide, 0.8 mM $CuSO_4$, 0.5 mM

https://dx.doi.org/10.1021/acssensors.9b02126
ACS Sens. XXXX, XXX, XXX−XXX

sodium ascorbate, and 0.1 mM tris(benzyltriazolylmethyl)amine (TBTA) or tris(3-hydroxypropyltriazolylmethyl)amine (THPTA) (Tables S1 and S2). In the case of Lys-terminated BDD, 9-fluorenylmethoxycarbonyl (Fmoc)-lysine(N_3)-OH was reacted in 50% ethanol as above, and the Fmoc group was then removed in the presence of 20% piperidine/*N*,*N*-dimethylformamide. The substrate was washed with water, ethanol, and acetone. After drying under N_2 gas, the obtained peptide-terminated BDD substrate was used for the electrochemical measurements within a few days.

Blocking Properties of Peptide-Terminated BDD. The cyclic voltammetry (CV) of ferrocene oxidation after the peptide modification step was recorded to characterize the blocking properties of the peptide layer on the BDD electrode. CVs between −0.2 and +0.8 V (versus Ag/AgCl) were recorded in 100 mM Na_2SO_4 containing 10 mM $K_3[Fe(CN)_6]$ with a scan rate of 100 mV/s (Figure 1C).

Peptide Density of Peptide on the BDD Surface. Surface coverage by the peptide (peptide density) was estimated using a ferrocenyl peptide-terminated BDD electrode.[33] A ferrocenyl peptide dimer was immobilized by the click reaction, as described for the peptide dimer. The three-electrode configuration was assembled with the ferrocenyl peptide-terminated BDD electrode (2.08 cm diameter), and then CVs were measured in phosphate-buffered saline (PBS; pH 7.4) with a scan rate of 200 mV/s between about +0.2 and +0.5 V (vs Ag/AgCl) (Figure S3).

The total coverage of the BDD surface by the peptide (Γ_{pep}, mol/cm^2) was determined from the integration of the area under the oxidation peak at low scan rates yielding the charge passed (Q, C/cm^2) according to the equation $\Gamma_{pep} = Q/(nFA)$,[35] where n is the number of electrons involved in the reaction (ferrocene, 1), F is the Faraday constant (96 485 C/mol), and A is the electroactive surface area of the peptide-terminated BDD electrode. The peptide density (pmol/cm^2) was obtained from the surface coverage, and the number of ferrocenyl groups in the peptide. The data are average values ± standard deviations of three independent experiments.

Detection of HA and IFV by EIS. The three-electrode configuration was assembled with a peptide-terminated BDD electrode (1.8 mm diameter, Figure 3A), and 50 μL of a solution consisting of HA, bovine serum albumin (BSA), or IFV in PBS (pH 7.4) for 15 min (HA and BSA) or 45 min (IFV) was incubated with the electrode. The electrode was washed three times with PBS, and a mixed solution (2 mL) of 5 mM $K_4[Fe(CN)_6]$ and 5 mM $K_3[Fe(CN)_6]$ in PBS was poured into the electrochemical cell assembly. EIS was measured at equilibrium or open-circuit potential without bias voltage in the frequency range from 5 Hz to 50 kHz with a 25 mV amplitude.[29,36] R_{ct} was defined as the diameter of the semicircle in the Nyquist plots.[37] Due to variations in the R_{ct} value between plots of the electrode, ΔR_{ct} was corrected with ΔR_{ct} in PBS (R_{ct0}). The normalized $\Delta R_{ct}/R_{ct0}$ values were plotted against a logarithmic scale of IFV concentration. After linear fitting, the LOD was calculated according to the equation LOD = 3.3 × SD/slope, where SD is the standard deviation at the lowest IFV concentration (typically 3 pfu).[15,38]

RESULTS AND DISCUSSION

Design of Peptide Dendrimers. HA from IFV recognizes sialylglycoconjugate receptors on the cell surface at the initial step of infection.[16,17] Peptide-based materials, which are derived from natural and artificial peptides, are viable alternatives to ligands and antibodies.[39] The pentapeptide showed receptor mimicry in place of the sialic acid-conjugated glycan; therefore, the peptide-terminated electrode had the potential to be applied as a universal biosensor against other subtypes of IFVs. To capture IFV, we identified a pentapeptide, Ala-Arg-Leu-Pro-Arg, that can bind to the receptor-binding site of HA.[24] The peptide-conjugated lipid has the ability to capture HA and IFV on the lipid membrane.[40] In addition, more than 20 pfu of human H1N1 and H3N2 IFVs were previously detected electrochemically by a peptide dimer immobilized on the BDD surface.[29]

In the present study, the effective immobilization of the peptide onto the electrode was investigated for electrochemical detection. To improve the affinity of the peptide for HA from IFV, divalent and tetravalent peptide dendrimers (dimers and tetramers) with a branched lysine (Lys) core were prepared (Figure 1).[25,27,41] The peptide dendrimers had a biotinyl side chain at the carboxyl terminal of the Lys core, and the affinity of the peptide dendrimer for HAs was determined by the avidin-biotin-peroxidase complex (ABC) method (Supporting Information). The affinity of dendrimers for HAs increased as the dendrimer generation increased; the affinity of the dimers and tetramers for H1 HA was five times (the dissociation constant (K_d), 14 μM dimer) and 185 times (0.4 μM tetramer) greater than that of the monomer (74 μM monomer), respectively (Figure S4A and Table S3).[25] This tendency for the affinity to increase was also found for H3 HA.

pH-Dependent Binding of Peptide Dendrimers. Conformational changes in HA occur under a low pH (generally, pH 6 or lower), which results in membrane fusion with viral and endosomal membranes.[42] Because the binding ability of the peptide to HA is thought to change according to changes in pH, the optimal pH for the peptide−HA interaction was determined by the ABC method. The amount of peptide tetramer bound to H1 HA increased depending on the peptide concentration (Figure S4B), and the K_d values of the peptide tetramer bound to H1 and H3 HAs were determined from reciprocal plots based on the Langmuir adsorption isotherm.[43] The K_d values of the tetramers for H1 and H3 HAs were 0.3−0.6 μM at pH 6.5−7.4, and the peptide dendrimer showed the highest binding affinity at around pH 7 (Figure S4C and Table S3).

Preparation of the Peptide-Terminated BDD Electrode. Immobilization of the peptide dendrimer was performed by the click reaction between the azide group-conjugated dendrimer and the alkyne-terminated BDD surface, as established previously.[29] Instead of a biotin group, an azide group (N_3) was introduced to the Lys side chain (Figure 1A), and an alkyne-terminated BDD electrode was prepared as described previously (Figure S2). Briefly, a thin BDD film was deposited onto an Si(111) wafer, and the triisopropylsilyl-protected phenylacetylene moiety was immobilized by electroreduction. After the deprotection of the triisopropylsilyl group, alkyne termination was confirmed by CV.

A click reaction of the alkyne-terminated BDD electrode and the azide-conjugated peptide dimer was carried out with different peptide concentrations (1 or 26 μM), ligands (TBTA or THPTA), and methanol contents (0 or 50%; Figure 1B, Tables S1 and S2). Based on the solubility of the peptides in water, TBTA or THPTA, a water-soluble derivative of TBTA was used as a stabilizing ligand for the Cu(I) catalyst in 50% methanol or water, respectively. Figure 1C shows the typical CVs of $[Fe(CN)_6]^{3-/4-}$, using BDD electrodes before and after peptide modification. Compared with the alkyne-terminated electrode, the peak potential separation of CVs between the oxidation and reduction reactions was larger, and the peak heights decreased. These results indicated that bulky peptide groups blocked electron transfer between BDD and $[Fe(CN)_6]^{3-/4-}$ in solution.

Estimation of Peptide Density Terminated on the BDD Surface. To evaluate detection ability, peptide dendrimers were terminated on the electrode at different

https://dx.doi.org/10.1021/acssensors.9b02126
ACS Sens. XXXX, XXX, XXX−XXX

Table 1. Peptide Density According to Click Reaction Conditions

code	[peptide dimer] (μM)	ligand	solvent	peptide density (pmol/cm^2)[a]	estimated peptides in a square of 100 nm
TBTA-1	1	TBTA	50% MeOH	0.11 ± 0.01	6.6
TBTA-26	26	TBTA	50% MeOH	0.26 ± 0.01	16
TBTA-100	100	TBTA	50% MeOH	2.1 ± 0.6	127
THPTA-1	1	THPTA	water	3.6 ± 0.4	217
THPTA-26	26	THPTA	water	5.6 ± 0.1	337

[a]The data are average values ± standard deviations (n = 3).

densities. The density of the peptide dendrimer on the BDD electrode was estimated using a ferrocene-conjugated peptide (Figure S3A).[33,36,44] The CV of the ferrocenyl peptide dimer-reacted BDD electrode was measured in PBS (Figure S3B). The anodic and cathodic peak current densities (i_{pa} and i_{pc}, respectively) were proportional to the potential sweep rate, and the i_{pa}/i_{pc} ratio was close to unity, indicating a ferrocene/ferrocenium redox process controlled by charge-transfer kinetics. These characteristics indicated that the ferrocenyl peptide was immobilized on the BDD surface.[29]

To obtain peptide density, the surface coverage of the peptide was determined by the integration of an oxidation current peak between 0.21 and 0.52 V (Figure S3B). We obtained four BDD electrodes with different peptide densities between 0.11 ± 0.01 and 5.6 ± 0.1 pmol/cm^2 (Table 1). The peptide density of the electrode that reacted with THPTA (3.6 and 5.6 pmol/cm^2) was an order of magnitude higher than that with TBTA (0.11 and 0.26 pmol/cm^2), potentially because of the solubility of the peptide in water. Because the peptide sequence used here was highly soluble in water, the reaction using THPTA was preferred to that using TBTA. However, the reaction using TBTA could be useful when the peptide sequence was more hydrophobic.[45]

Based on the peptide densities of 0.11, 0.26, 3.6, and 5.6 pmol/cm^2, the number of peptides terminated in an area of 100 × 100 nm^2 (i.e., 10 000 nm^2) was calculated to be 6.6, 16, 217, and 337 molecules, respectively (Table 1 and Figure S3C). Because the size of IFV particles was 80−120 nm in diameter, one viral particle could interact with 6.6−337 peptides on the BDD surface.

Peptide Density-Dependent HA Detection by the Peptide Dimer. When biomacromolecules, such as HA and IFV, are bound to the peptide, electron transfer between the redox probe and electrode is limited.[10,46] This limitation is detected by EIS as an increase in charge-transfer resistance (R_{ct}) on the electrode surface. To optimize the sensitivity of the electrode, electrodes were prepared with dendrimer densities of 2−50 times higher than that used previously.[29] The peptide-terminated BDD surface was incubated with 5−500 nM HA in PBS for 15 min, washed with PBS, and subjected to EIS using 5 mM $[Fe(CN)_6]^{3-/4-}$ in PBS as a redox probe, as described previously (Figures 2 and 3A). Figure 3B shows typical Nyquist plots for H1 HA using the peptide-terminated BDD electrode with a peptide density of 5.6 pmol/cm^2. The R_{ct} value, i.e., the diameter of the semicircle in the Nyquist plots, increased as the protein concentration increased. The value responding to the binding of H1 HA was higher than that of BSA at all protein concentrations (Figure 4). The binding selectivity, which demonstrated that the R_{ct} ratio of HA to BSA was 1 or more, was observed using electrodes with peptide densities of 0.11−5.6 pmol/cm^2. However, the value responding to the binding of BSA to BDD with peptide densities of 0.26−3.6 pmol/cm^2 was

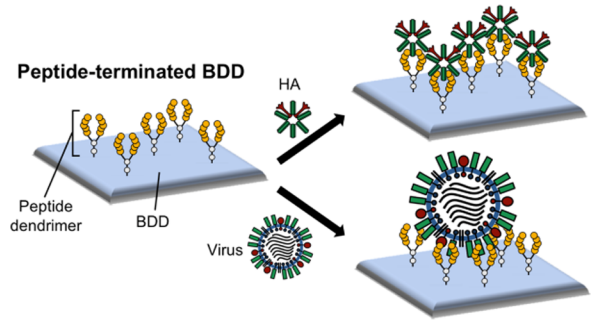

Figure 2. Schematic representation of HA and virus binding to peptide-terminated BDD.

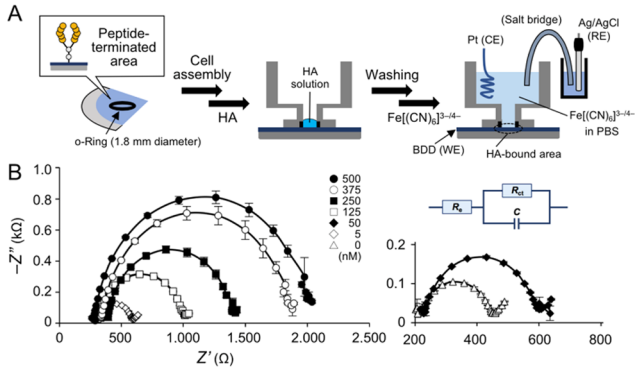

Figure 3. HA detection using peptide dimer-terminated BDD electrodes. (A) Schematic illustration of the measurement of HA with peptide-terminated BDD electrodes. After assembly of electrochemical cell parts with the BDD electrode, the peptide-terminated surface was incubated with the HA solution. After washing, EIS was performed using $Fe[(CN)_6]^{3-/4-}$ in PBS. WE, working electrode; CE, counter electrode; RE, reference electrode. (B) Representative Nyquist plots of H1 HA on the peptide-terminated BDD electrode with a peptide density of 5.6 pmol/cm^2. Inset, electrical equivalent circuit.

unignorable for the detection of H1 HA. The adsorption of negatively charged BSA onto the BDD electrode at neutral pH is supposed to be induced by a positive peptide charge derived from two arginine residues, and the decreased impedance at high adsorption may be explained using a density-packed protein monolayer model.[47] This model could provide an explanation of the decreased impedance response of the BDD electrode when exposed to high protein concentration. This phenomenon is induced by the change in orientations of protein molecules on a solid surface; a loosely packed monolayer of proteins is generated on the BDD surface at high concentrations, compared with a densely packed monolayer on reduced graphene oxide.

Peptide Density-Dependent IFV Detection by the Peptide Dimer. The peptide-terminated BDD surface was

https://dx.doi.org/10.1021/acssensors.9b02126
ACS Sens. XXXX, XXX, XXX−XXX

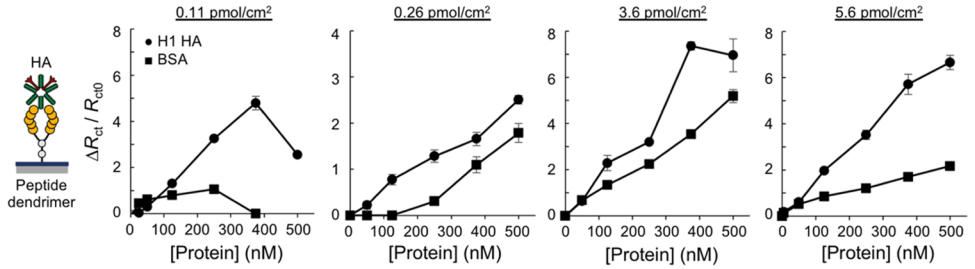

Figure 4. Relative change in R_{ct} (ΔR_{ct}) as a function of HA concentration in PBS. R_{ct0}, ΔR_{ct} in PBS. [protein] = 0, 5, 50, 125, 250, 375, or 500 nM. Peptide density = 0.11, 0.26, 3.6, and 5.6 pmol/cm^2. A plot of $\Delta R_{ct}/R_{ct0}$ using an electrode with a peptide density of 0.11 pmol/cm^2 was reproduced in part with permission from ref 29. Copyright 2016 National Academy of Sciences. The data are average values ± standard deviations (n = 3).

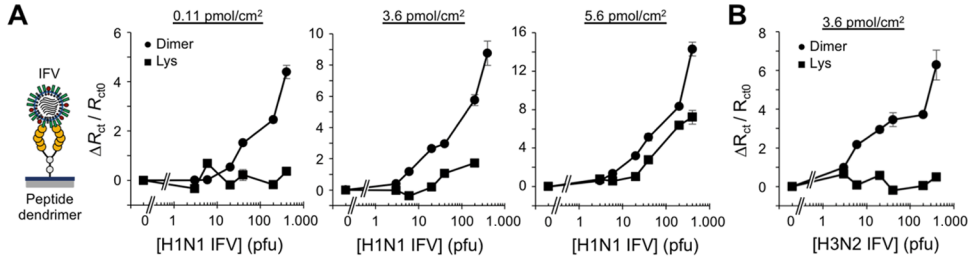

Figure 5. IFV detection using peptide dimer-terminated BDD electrodes. (A) Dependence of ΔR_{ct} on the number of H1N1 IFVs in PBS using electrodes with different peptide densities. The peptide-terminated surface was incubated with the IFV solution, and EIS was performed using $Fe[(CN)_6]^{3-/4-}$ in PBS. The IFV solution contained 0, 3, 6, 20, 40, 200, and 400 pfu in 50 μL PBS. A plot of $\Delta R_{ct}/R_{ct0}$ using an electrode with a peptide density of 0.11 pmol/cm^2 was reproduced with permission from ref 29. Copyright 2016 National Academy of Sciences. (B) Dependence of ΔR_{ct} on the number of H3N2 IFVs in PBS using the electrode with a peptide density of 3.6 pmol/cm^2. The IFV subtypes were A/Puerto Rico/8/34 (H1N1) and A/Aichi/2/68 (H3N2). The data are average values ± standard deviations (n = 3).

Table 2. Limit and Range of IFV Detection

peptide dendrimer	peptide density (pmol/cm^2)	viral subtype[a]	solution	R_{ct0} (Ω)	limit of detection (pfu)	range of detection (pfu)[b]
2 mer	0.11	human H1N1	PBS	2180 ± 3	12.5	20−400[29]
2 mer	3.6	human H1N1	PBS	156 ± 2	3.3	6−400
2 mer	3.6	human H3N2	PBS	98 ± 4	0.91	6−400
4 mer	0.11	human H1N1	PBS	1066 ± 98	15	20−400
4 mer	3.6	human H1N1	PBS	267 ± 6	3.0	6−200
4 mer	3.6	human H1N1	BSA/PBS	68 ± 6	0.33	3−400
4 mer	3.6	human H1N1	HSA/PBS	74 ± 2	0.60	3−400
4 mer	3.6	duck H5N3	PBS	48 ± 1	0.13	3−400
4 mer	3.6	duck H7N1	PBS	126 ± 5	0.38	3−400
4 mer	3.6	duck H9N2	PBS	63 ± 1	6.7	3−400

[a]A/Puerto Rico/8/34 (H1N1); A/Aichi/2/68 (H3N2); A/duck/Hong Kong/820/1980 (H5N3); A/duck/Hong Kong/301/1978 (H7N1); A/duck/Hong Kong/448/1978 (H9N2). [b]Significantly detected compared with the Lys-terminated BDD electrode (0 pmol/cm^2).

incubated with IFV (3−400 pfu) in 50 μL PBS for 45 min, and the binding of IFV was then detected by EIS. The R_{ct} value increased as the IFV particle number and peptide density increased, and the binding of the H1N1 IFV A/Puerto Rico/8/34 to peptide-terminated BDD was higher than that to a Lys-terminated BDD without a sialic acid-mimic peptide (Figure 5A). The electrode with a peptide density of 3.6 pmol/cm^2 was chosen for further investigation because the R_{ct} value for Lys-terminated BDD (0 pmol/cm^2) was not significantly increased in this electrode. The binding of another H3N2 subtype, A/Aichi/2/68, to peptide-terminated BDD is shown in Figure 5B.

For both subtypes of viruses, a virus with only 6 pfu was significantly detected; the sensitivity of the electrode with a peptide density of 3.6 pmol/cm^2 was about 3 times higher than that of the previous electrode (0.11 pmol/cm^2, detectable between 20 and 400 pfu).[29] The LODs of H1N1 and H3N2 were 3.3 and 0.91 pfu, respectively (Table 2).

Characterization of IFV Binding to Peptide-Terminated BDD. The sensitivity of the peptide-terminated BDD electrode was very high. However, the validity of this sensitivity is not clear. Scanning electron microscopy (SEM) of a peptide-terminated BDD after IFV incubation is shown in Figure S5A. The crystal surface of bare BDD was smooth, whereas particles of around 100 nm in size were observed after IFV incubation (four particles observed in a 5 × 5 μm^2 area). The particles were assigned to IFVs based on the known diameter of IFV particles (80−120 nm).[48] Other smaller particles of approximately 10−20 nm were observed and may represent debris from viruses and/or other types of albumins. The size of IFVs was also measured by dynamic light scattering. The particle size of IFV was approximately 200 nm, as previously reported,[49] and the small proteins identified in the SEM

https://dx.doi.org/10.1021/acssensors.9b02126
ACS Sens. XXXX, XXX, XXX−XXX

imaging were observed as approximately 50 nm particles (Figure S5B).

Our results showed evidence of binding to the BDD surface after incubation with 400 pfu of H3N2 IFV (50 μL) in a circular area with a diameter of 1.8 mm (2.54 mm^2). Based on a particle-to-pfu ratio of 50−100, 400 pfu corresponds to 40 000 viral particles.[50,51] If all particles are bound to this surface, 0.4 particles should be observed in a 5 × 5 μm^2 area. In our study, four particles were observed in a 5 × 5 μm^2 area (Figure S5A). Thus, although the particle-to-pfu ratio used may not be completely accurate, this estimation supported the results of IFV detection using the peptide-terminated BDD electrode shown in the current study.

To confirm that IFV binding was mediated by the peptide dendrimer, IFVs were incubated with peptide-terminated BDD in the presence of a free peptide dimer. The R_{ct} values decreased as the peptide concentration increased (Figure S5C). These results suggested that R_{ct} responses were related to the interactions between the IFV and peptide dendrimer on the BDD surface.

HA and IFV Detection by the Peptide Tetramer. The tetravalent peptide dendrimer showed the highest affinity for HAs (Table S3). The tetramer (Figure S1) was immobilized onto the BDD electrode under conditions (THPTA-1) in which the dimer-terminated electrode could be prepared with a peptide density of 3.6 pmol/cm^2 (Table 1). The binding of H1 HA in the range of 5−400 nM was clearly observed, whereas a very low level of BSA binding occurred (Figure 6A). Because

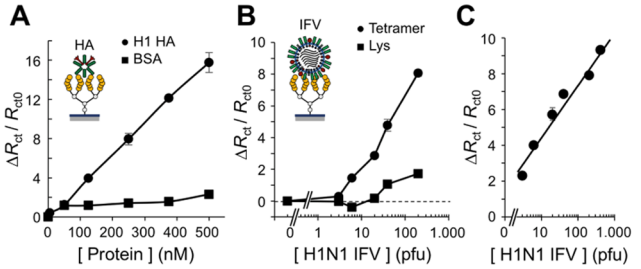

Figure 6. HA and IFV detection using peptide tetramer-terminated BDD electrodes. (A) Relative change in R_{ct} (ΔR_{ct}) as a function of H1 HA concentration in PBS. (B) ΔR_{ct} value as a function of the number of IFVs in PBS. IFV solution contained 0, 3, 6, 20, 40, or 200 pfu of H1N1 IFV (A/Puerto Rico/8/34) in 50 μL PBS. (C) H1N1 IFV detection in the presence of BSA (500 nM). Linear fitting with a logarithmic scale in the IFV concentration range from 3 to 400 pfu in 50 μL PBS. The LOD was calculated from the slope of the fitting and standard deviation of the $\Delta R_{ct}/R_{ct0}$ value at 3 pfu. The peptide density of the peptide tetramer-terminated BDD was 3.6 pmol/cm^2. The data are average values ± standard deviations (n = 3).

substantial binding of BSA was observed using the dimer-terminated electrode under these conditions (Figure 4), we found that the tetramer-terminated electrode showed better detection of HA than the dimer-terminated electrode.

More than 6 pfu virus was clearly detected using the tetramer-terminated electrode, indicating highly sensitive detection of H1N1 IFV (Figure 6B). Furthermore, in the presence of BSA or human serum albumin (HSA), 3 pfu virus was detected, demonstrating that the electrode also showed the highest sensitivity for H1N1 IFV (Figure 6C). This was because the medium supplemented with serum albumin is often used for the collection of the virus from specimens to stabilize the viruses.[4] The LODs of this electrode in the absence and presence of BSA were 3.0 and 0.33 pfu/sample solution (50 μL), respectively (Table 2), which was comparable to those using an antibody-based BDD electrode (5−10 pfu/sample)[15] and real-time polymerase chain reaction (1.4−35 pfu/mL; calculated from 2 to 50 50% tissue culture infective doses [$TCID_{50}$]/mL).[52] Although the affinity of the peptide tetramer was 8−35 times higher than that of the dimer (Table S3), no increase was observed in the sensitivity of the peptide tetramer-terminated electrode with peptide densities of either 0.11 or 3.6 pmol/cm^2 (Table 2). This may be because the density is more important for sensitivity and/or the electrode of the 3.6 pmol/cm^2 density had already delivered the highest performance for sensitivity.

Avian IFV Detection by the Peptide Tetramer. Human infections with avian viruses, such as H5N1 and H7N9 substrains, induce severe diseases with high mortality rates, 53.5% (483/903 cases) and 33.8% (47/139 cases), respectively.[53,54] To prevent the circulation of avian virus infection in humans and also to detect the emergence of novel influenza viruses that could cause pandemics, public health surveillance of influenza virus is needed on a global scale. Avian viruses H5N3, H7N1, and H9N2 generated from MDCK cells were subjected to BDD detection. The peptide tetramer was immobilized onto the BDD electrode with a density of 3.6 pmol/cm^2. Similar to human IFVs, the peptide-terminated BDD surface was incubated with avian IFV (3−400 pfu), and the binding of IFV was then detected by EIS. Using the tetramer-terminated BDD electrode, more than 3 pfu H5N3 virus was clearly detected (Figure 7), although no detection of

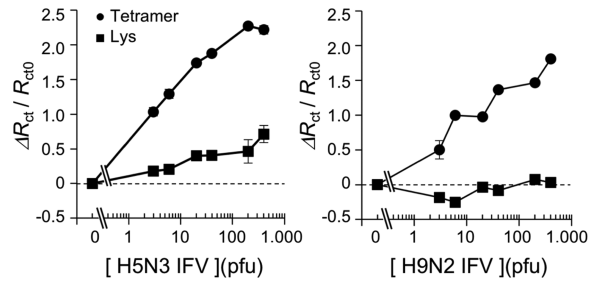

Figure 7. Avian IFV detection using peptide tetramer-terminated BDD electrodes. The ΔR_{ct} value as a function of the number of IFVs in PBS. IFV solution contained 0, 3, 6, 20, 40, 200, or 400 pfu of H5N3 (A/duck/Hong Kong/820/1980) and H9N2 (A/duck/Hong Kong/448/1978) IFVs in 50 μL PBS. The peptide density of the peptide tetramer-terminated BDD was 3.6 pmol/cm^2. The data are average values ± standard deviations (n = 3).

the avian virus was observed with the dimer-terminated BDD electrode (data not shown). The relative $\Delta R_{ct}/R_{ct0}$ value was lower than that of human IFVs, but the tetramer-terminated BDD electrode showed excellent LODs in the range of 0.13−6.7 pfu for avian IFV detection (Table 2). These results indicated that the peptide tetramer-terminated BDD electrode was useful for the detection of both human and avian IFVs.

There may be several factors influencing the sensitivities of IFV detection. One of the reasons for these differences in the intensities of relative $\Delta R_{ct}/R_{ct0}$ values between human and avian viruses may be due to interfering substances in IFV stocks (see the Experimental Section). For example, the amounts of total proteins, including defective interfering particle and unidentified proteinaceous molecules in the human IFV stocks from chicken eggs (11 mg/mL), were

https://dx.doi.org/10.1021/acssensors.9b02126
ACS Sens. XXXX, XXX, XXX−XXX

approximately 10-times greater than the avian IFV stocks from MDCK cells (1.1−1.3 mg/mL). Here, the amount of 10% fetal bovine serum (FBS) used for cell culture was 2.4 mg/mL, and the total proteins detected in the solution of human IFVs corresponded to 0.01−1.2% FBS. In general, the contents of unidentified protein, mucins, and other molecules should vary according to the method of collection (swab, wash, and aspirate) and the site of collection (nasal, nasopharynx, throat, etc.) of specimen collected from patients.[55] To perform accurate detection with high sensitivity, interfering molecules in specimens should be removed by pretreatment before detection. Indeed, an extraction process of viral antigens from specimens is included in protocols for commercially available rapid influenza diagnostic tests as pretreatment.[56] Therefore, we need to identify the factors influencing IFV detection and then develop a protocol to remove interfering molecules in specimens. Recent studies showed that mucin expressed on the surface of epithelial cells in the respiratory tract modulates the infection efficiency of IFV, and the expression of mucins is induced by IFV infection.[57,58] Cough aerosol particles produced from patients with influenza can contain not only IFV but also large amounts of mucins. The minimum infectious aerosol dose was determined by exposure of human volunteers to titrated aerosolized IFV suspensions.[59,60] Approximately 50% human infectious dose of virus per person ranged from 0.7 to 88 pfu (1−126 $TCID_{50}$). Thus, although we may need to remove mucins from cough aerosol particles, our peptide-based biosensor has sufficient sensitivity to detect the harmful concentration of IFVs in the air.

The peptide sequence, ARLPR, used here was chosen based on its binding affinity for both H1N1 and H3N2 HAs among the sialyloligosaccharide receptor-mimic peptides identified by phage-display selection. However, other peptide sequences, e.g., RTMVHPK and VHPKPAQP, showed inhibitory activity against H1N1 and H3N2 subtypes, respectively,[32] suggesting that these peptides have different affinities for HAs among subtypes (and strains) of IFVs. There are two reasons to explain this difference. First, these peptides may have some kinds of interaction with antigenic site(s) around the receptor-binding site, because IFV is classified into subtypes based on the antigenicity of antibodies against the HA surface. Another reason is that these peptides may mimic not only a sialic acid moiety but also a second galactose (and more) moiety from the nonreducing end in sialylglycoconjugates. The distinction of the IFV subtypes may not be essential for clinical practice, but identification of subtypes of IFV should be useful for surveillance. Electrodes terminated with peptides selective for IFV subtypes (and strains) could find application in the detection system for clinical surveillance.

CONCLUSIONS

Several types of antibodies against viral proteins, such as M1 protein and HA, have been used for the detection of IFVs. Although the affinity of peptides for target molecules is lower than that of antibodies, the peptide-terminated BDD electrode developed in the present study (3−400 pfu/sample) had a similar high sensitivity to antibody-terminated BDD electrodes (5−10 pfu/sample).[15] Because the receptor-binding site is conserved in other subtypes of IFVs, molecular mimicry of receptor function by peptides is a promising strategy for viral detection without using sialylglycoconjugates. The circulation of highly pathogenic H5N1 and H7N9 viruses is a major concern; however, these viruses still contains a sialyl galactose structure with α2−3 (for avians) and α2−6 linkages (for humans).[2,17,61] Thus, to counter the antigenic drift of viruses and the emergence of new types of viruses, our designed peptides could be promising candidates to replace antibodies. Such a peptide-based biosensor could be applied for the early diagnosis of influenza and for the surveillance of IFVs for humans, avians, and other animals.

ASSOCIATED CONTENT

Supporting Information

The Supporting Information is available free of charge at https://pubs.acs.org/doi/10.1021/acssensors.9b02126.

ABC method for binding of the peptide to HA; characterization of IFV on the BDD surface; affinity of peptide dendrimers for H1 and H3 HAs determined by the ABC method; typical conditions for the click reaction of peptide and alkene on the BDD electrode using TBTA and THPTA; determination of sialic acid-mimic peptide tetramer with an azide group; preparation of the alkyne-terminated BDD electrode; determination of peptide density on the BDD electrode; affinity of peptide dendrimers for HAs; and characterization of IFV binding to the peptide-terminated BDD electrode (PDF)

AUTHOR INFORMATION

Corresponding Author

Toshinori Sato − *Department of Biosciences and Informatics, Faculty of Science and Technology, Keio University, Yokohama, Kanagawa 223-8522, Japan;* orcid.org/0000-0002-4429-6101; Email: sato@bio.keio.ac.jp

Authors

Teruhiko Matsubara − *Department of Biosciences and Informatics, Faculty of Science and Technology, Keio University, Yokohama, Kanagawa 223-8522, Japan;* orcid.org/0000-0002-8006-4324

Michiko Ujie − *Department of Biosciences and Informatics, Faculty of Science and Technology, Keio University, Yokohama, Kanagawa 223-8522, Japan*

Takashi Yamamoto − *Department of Chemistry, Faculty of Science and Technology, Keio University, Yokohama, Kanagawa 223-8522, Japan;* orcid.org/0000-0002-4252-8132

Yasuaki Einaga − *Department of Chemistry, Faculty of Science and Technology, Keio University, Yokohama, Kanagawa 223-8522, Japan; JST-ACCEL, Tokyo 102-0075, Japan;* orcid.org/0000-0001-7057-4358

Tomo Daidoji − *Department of Infectious Diseases, Graduate School of Medical Science, Kyoto Prefectural University of Medicine, Kyoto 602-8566, Japan*

Takaaki Nakaya − *Department of Infectious Diseases, Graduate School of Medical Science, Kyoto Prefectural University of Medicine, Kyoto 602-8566, Japan*

Complete contact information is available at: https://pubs.acs.org/10.1021/acssensors.9b02126

Author Contributions

⊥T.M. and M.U. contributed equally to this work.

Notes

The authors declare no competing financial interest.

https://dx.doi.org/10.1021/acssensors.9b02126
ACS Sens. XXXX, XXX, XXX−XXX

■ ACKNOWLEDGMENTS

The authors would like to express their sincere thanks to Mr. M.Takasaki for technical assistance for SEM measurement. This work was supported in part by AMED (grant No. JP19hm0102056 to T.S.), and Japan Society for the Promotion of Science KAKENHI (grant No. JP15K01806 to T.M.).

■ REFERENCES

(1) Paules, C.; Subbarao, K. Influenza. *Lancet* **2017**, *390*, 697−708.
(2) Webster, R. G.; Govorkova, E. A. Continuing challenges in influenza. *Ann. N. Y. Acad. Sci.* **2014**, *1323*, 115−139.
(3) von Itzstein, M. The war against influenza: discovery and development of sialidase inhibitors. *Nat. Rev. Drug Discovery* **2007**, *6*, 967−974.
(4) Sakai-Tagawa, Y.; Ozawa, M.; Tamura, D.; Le, M.; Nidom, C. A.; Sugaya, N.; Kawaoka, Y. Sensitivity of influenza rapid diagnostic tests to H5N1 and 2009 pandemic H1N1 viruses. *J. Clin. Microbiol.* **2010**, *48*, 2872−2877.
(5) Hayden, F. G.; Osterhaus, A. D.; Treanor, J. J.; Fleming, D. M.; Aoki, F. Y.; Nicholson, K. G.; Bohnen, A. M.; Hirst, H. M.; Keene, O.; Wightman, K. Efficacy and safety of the neuraminidase inhibitor zanamivir in the treatment of influenzavirus infections. GG167 Influenza Study Group. *N. Engl. J. Med.* **1997**, *337*, 874−880.
(6) Ngom, B.; Guo, Y.; Wang, X.; Bi, D. Development and application of lateral flow test strip technology for detection of infectious agents and chemical contaminants: a review. *Anal. Bioanal. Chem.* **2010**, *397*, 1113−1135.
(7) Sakurai, A.; Takayama, K.; Nomura, N.; Munakata, T.; Yamamoto, N.; Tamura, T.; Yamada, J.; Hashimoto, M.; Kuwahara, K.; Sakoda, Y.; Suda, Y.; Kobayashi, Y.; Sakaguchi, N.; Kida, H.; Kohara, M.; Shibasaki, F. Broad-spectrum detection of H5 subtype influenza A viruses with a new fluorescent immunochromatography system. *PLoS One* **2013**, *8*, No. e76753.
(8) Sakurai, A.; Takayama, K.; Nomura, N.; Kajiwara, N.; Okamatsu, M.; Yamamoto, N.; Tamura, T.; Yamada, J.; Hashimoto, M.; Sakoda, Y.; Suda, Y.; Kobayashi, Y.; Kida, H.; Shibasaki, F. Fluorescent Immunochromatography for Rapid and Sensitive Typing of Seasonal Influenza Viruses. *PLoS One* **2015**, *10*, No. e0116715.
(9) Einaga, Y. Diamond electrodes for electrochemical analysis. *J. Appl. Electrochem.* **2010**, *40*, 1807−1816.
(10) Luong, J. H.; Male, K. B.; Glennon, J. D. Boron-doped diamond electrode: synthesis, characterization, functionalization and analytical applications. *Analyst* **2009**, *134*, 1965−1979.
(11) Fujishima, A.; Einaga, Y.; Rao, T. N.; Tryk, D. A. *Diamond Electrochemistry*; Elsevier-BKC: Tokyo, 2005.
(12) Hassen, W. M.; Duplan, V.; Frost, E.; Dubowski, J. J. Quantitation of influenza A virus in the presence of extraneous protein using electrochemical impedance spectroscopy. *Electrochim. Acta* **2011**, *56*, 8325−8328.
(13) Nidzworski, D.; Pranszke, P.; Grudniewska, M.; Krol, E.; Gromadzka, B. Universal biosensor for detection of influenza virus. *Biosens. Bioelectron.* **2014**, *59*, 239−242.
(14) Sepunaru, L.; Plowman, B. J.; Sokolov, S. V.; Young, N. P.; Compton, R. G. Rapid electrochemical detection of single influenza viruses tagged with silver nanoparticles. *Chem. Sci.* **2016**, *7*, 3892−3899.
(15) Nidzworski, D.; Siuzdak, K.; Niedzialkowski, P.; Bogdanowicz, R.; Sobaszek, M.; Ryl, J.; Weiher, P.; Sawczak, M.; Wnuk, E.; Goddard, W. A., 3rd; Jaramillo-Botero, A.; Ossowski, T. A rapid-response ultrasensitive biosensor for influenza virus detection using antibody modified boron-doped diamond. *Sci. Rep.* **2017**, *7*, No. 15707.
(16) Gamblin, S. J.; Skehel, J. J. Influenza hemagglutinin and neuraminidase membrane glycoproteins. *J. Biol. Chem.* **2010**, *285*, 28403−28409.
(17) Suzuki, Y. Sialobiology of influenza: molecular mechanism of host range variation of influenza viruses. *Biol. Pharm. Bull.* **2005**, *28*, 399−408.
(18) Zhao, N.; Martin, B. E.; Yang, C. K.; Luo, F.; Wan, X. F. Association analyses of large-scale glycan microarray data reveal novel host-specific substructures in influenza A virus binding glycans. *Sci. Rep.* **2015**, *5*, No. 15778.
(19) Stevens, J.; Blixt, O.; Glaser, L.; Taubenberger, J. K.; Palese, P.; Paulson, J. C.; Wilson, I. A. Glycan microarray analysis of the hemagglutinins from modern and pandemic influenza viruses reveals different receptor specificities. *J. Mol. Biol.* **2006**, *355*, 1143−1155.
(20) Hideshima, S.; Hinou, H.; Ebihara, D.; Sato, R.; Kuroiwa, S.; Nakanishi, T.; Nishimura, S.; Osaka, T. Attomolar detection of influenza A virus hemagglutinin human H1 and avian H5 using glycan-blotted field effect transistor biosensor. *Anal. Chem.* **2013**, *85*, 5641−5644.
(21) Hushegyi, A.; Bertok, T.; Damborsky, P.; Katrlik, J.; Tkac, J. An ultrasensitive impedimetric glycan biosensor with controlled glycan density for detection of lectins and influenza hemagglutinins. *Chem. Commun.* **2015**, *51*, 7474−7477.
(22) Hushegyi, A.; Pihikova, D.; Bertok, T.; Adam, V.; Kizek, R.; Tkac, J. Ultrasensitive detection of influenza viruses with a glycan-based impedimetric biosensor. *Biosens. Bioelectron.* **2016**, *79*, 644−649.
(23) Zhang, X.; Dhawane, A. N.; Sweeney, J.; He, Y.; Vasireddi, M.; Iyer, S. S. Electrochemical assay to detect influenza viruses and measure drug susceptibility. *Angew. Chem., Int. Ed.* **2015**, *54*, 5929−5932.
(24) Matsubara, T.; Onishi, A.; Saito, T.; Shimada, A.; Inoue, H.; Taki, T.; Nagata, K.; Okahata, Y.; Sato, T. Sialic acid-mimic peptides as hemagglutinin inhibitors for anti-influenza therapy. *J. Med. Chem.* **2010**, *53*, 4441−4449.
(25) Matsubara, T.; Onishi, A.; Saito, T.; Yamaguchi, D.; Sato, T. Multivalent Effect in Influenza Hemagglutinin-Binding Activity of Sugar-Mimic Peptide. *Kobunshi Ronbunshu* **2016**, *73*, 62−68.
(26) Hatano, K.; Matsubara, T.; Muramatsu, Y.; Ezure, M.; Koyama, T.; Matsuoka, K.; Kuriyama, R.; Kori, H.; Sato, T. Synthesis and influenza virus inhibitory activities of carbosilane dendrimers peripherally functionalized with hemagglutinin-binding Peptide. *J. Med. Chem.* **2014**, *57*, 8332−8339.
(27) Tam, J. P. Synthetic peptide vaccine design: synthesis and properties of a high-density multiple antigenic peptide system. *Proc. Natl. Acad. Sci. U.S.A.* **1988**, *85*, 5409−5413.
(28) Bray, B. L. Large-scale manufacture of peptide therapeutics by chemical synthesis. *Nat. Rev. Drug Discovery* **2003**, *2*, 587−593.
(29) Matsubara, T.; Ujie, M.; Yamamoto, T.; Akahori, M.; Einaga, Y.; Sato, T. Highly sensitive detection of influenza virus by boron-doped diamond electrode terminated with sialic acid-mimic peptide. *Proc. Natl. Acad. Sci. U.S.A.* **2016**, *113*, 8981−8984.
(30) Asahi, Y.; Yoshikawa, T.; Watanabe, I.; Iwasaki, T.; Hasegawa, H.; Sato, Y.; Shimada, S.; Nanno, M.; Matsuoka, Y.; Ohwaki, M.; Iwakura, Y.; Suzuki, Y.; Aizawa, C.; Sata, T.; Kurata, T.; Tamura, S. Protection against influenza virus infection in polymeric Ig receptor knockout mice immunized intranasally with adjuvant-combined vaccines. *J. Immunol.* **2002**, *168*, 2930−2938.
(31) Daidoji, T.; Watanabe, Y.; Ibrahim, M. S.; Yasugi, M.; Maruyama, H.; Masuda, T.; Arai, F.; Ohba, T.; Honda, A.; Ikuta, K.; Nakaya, T. Avian Influenza Virus Infection of Immortalized Human Respiratory Epithelial Cells Depends upon a Delicate Balance between Hemagglutinin Acid Stability and Endosomal pH. *J. Biol. Chem.* **2015**, *290*, 10627−10642.
(32) Matsubara, T.; Sumi, M.; Kubota, H.; Taki, T.; Okahata, Y.; Sato, T. Inhibition of influenza virus infections by sialylgalactose-binding peptides selected from a phage library. *J. Med. Chem.* **2009**, *52*, 4247−4256.
(33) Yamamoto, T.; Akahori, M.; Natsui, K.; Saitoh, T.; Einaga, Y. Controlled decoration of boron-doped diamond electrodes by electrochemical click reaction (e−CLICK). *Carbon* **2018**, *130*, 350−354.
(34) Natsui, K.; Yamamoto, T.; Akahori, M.; Einaga, Y. Photo-chromism-induced amplification of critical current density in

https://dx.doi.org/10.1021/acssensors.9b02126
ACS Sens. XXXX, XXX, XXX−XXX

superconducting boron-doped diamond with an azobenzene molecular layer. *ACS Appl. Mater. Interfaces* **2015**, *7*, 887−894.
(35) Leroux, Y. R.; Fei, H.; Noel, J. M.; Roux, C.; Hapiot, P. Efficient covalent modification of a carbon surface: use of a silyl protecting group to form an active monolayer. *J. Am. Chem. Soc.* **2010**, *132*, 14039−14041.
(36) Arya, S. K.; Kongsuphol, P.; Wong, C. C.; Polla, L. J.; Park, M. K. Label free biosensor for sensitive human influenza virus hemagglutinin specific antibody detection using coiled-coil peptide modified microelectrode array based platform. *Sens. Actuators, B* **2014**, *194*, 127−133.
(37) Yang, L.; Bashir, R. Electrical/electrochemical impedance for rapid detection of foodborne pathogenic bacteria. *Biotechnol. Adv.* **2008**, *26*, 135−150.
(38) Chavan, S. G.; Kim, D.; Hwang, J.; Choi, Y.; Hong, J. W.; Kim, J.; Lee, M. H.; Hwang, M. P.; Choi, J. Enhanced Detection of Infectious Pancreatic Necrosis Virus via Lateral Flow Chip and Fluorometric Biosensors Based on Self-Assembled Protein Nanoprobes. *ACS Sens.* **2019**, *4*, 2937−2944.
(39) Ladner, R. C.; Sato, A. K.; Gorzelany, J.; de Souza, M. Phage display-derived peptides as therapeutic alternatives to antibodies. *Drug Discovery Today* **2004**, *9*, 525−529.
(40) Matsubara, T.; Shibata, R.; Sato, T. Binding of Hemagglutinin and Influenza Virus to a Peptide-Conjugated Lipid Membrane. *Front. Microbiol.* **2016**, *7*, No. 468.
(41) Sadler, K.; Tam, J. P. Peptide dendrimers: applications and synthesis. *J. Biotechnol.* **2002**, *90*, 195−229.
(42) Fontana, J.; Cardone, G.; Heymann, J. B.; Winkler, D. C.; Steven, A. C. Structural changes in Influenza virus at low pH characterized by cryo-electron tomography. *J. Virol.* **2012**, *86*, 2919−2929.
(43) Matsubara, T.; Onishi, A.; Yamaguchi, D.; Sato, T. Heptapeptide ligands against receptor-binding sites of influ-enza hemagglutinin toward anti-influenza therapy. *Bioorg. Med. Chem.* **2016**, *24*, 1106−1114.
(44) Kondo, T.; Hoshi, H.; Honda, K.; Einaga, Y.; Fujishima, A.; Kawai, T. Photochemical Modification of a Boron-doped Diamond Electrode Surface with Vinylferrocene. *J. Phys. Chem. C* **2008**, *112*, 11887−11892.
(45) Chan, T. R.; Hilgraf, R.; Sharpless, K. B.; Fokin, V. V. Polytriazoles as copper(I)-stabilizing ligands in catalysis. *Org. Lett.* **2004**, *6*, 2853−2855.
(46) Szunerits, S.; Niedziolka-Jonsson, J.; Boukherroub, R.; Woisel, P.; Baumann, J. S.; Siriwardena, A. Label-free detection of lectins on carbohydrate-modified boron-doped diamond surfaces. *Anal. Chem.* **2010**, *82*, 8203−8210.
(47) Huang, Y.; Hara, A.; Terashima, C.; Fujishima, A.; Takai, M. Protein adsorption behavior on reduced graphene oxide and boron-doped diamond investigated by electrochemical impedance spectroscopy. *Carbon* **2019**, *152*, 354−362.
(48) Noda, T.; Sagara, H.; Yen, A.; Takada, A.; Kida, H.; Cheng, R. H.; Kawaoka, Y. Architecture of ribonucleoprotein complexes in influenza A virus particles. *Nature* **2006**, *439*, 490−492.
(49) Zhang, Z.; Schepens, B.; Nuhn, L.; Saelens, X.; Schotsaert, M.; Callewaert, N.; De Rycke, R.; Zhang, Q.; Moins, S.; Benali, S.; Mespouille, L.; Hoogenboom, R.; De Geest, B. G. Influenza-binding sialylated polymer coated gold nanoparticles prepared via RAFT polymerization and reductive amination. *Chem. Commun.* **2016**, *52*, 3352−3355.
(50) Martin, K.; Helenius, A. Transport of incoming influenza virus nucleocapsids into the nucleus. *J. Virol.* **1991**, *65*, 232−244.
(51) Marcus, P. I.; Ngunjiri, J. M.; Sekellick, M. J. Dynamics of biologically active subpopulations of influenza virus: plaque-forming, noninfectious cell-killing, and defective interfering particles. *J. Virol.* **2009**, *83*, 8122−8130.
(52) Jannetto, P. J.; Buchan, B. W.; Vaughan, K. A.; Ledford, J. S.; Anderson, D. K.; Henley, D. C.; Quigley, N. B.; Ledeboer, N. A. Real-time detection of influenza a, influenza B, and respiratory syncytial virus a and B in respiratory specimens by use of nanoparticle probes. *J. Clin. Microbiol.* **2010**, *48*, 3997−4002.
(53) Lai, S.; Qin, Y.; Cowling, B. J.; Ren, X.; Wardrop, N. A.; Gilbert, M.; Tsang, T. K.; Wu, P.; Feng, L.; Jiang, H.; Peng, Z.; Zheng, J.; Liao, Q.; Li, S.; Horby, P. W.; Farrar, J. J.; Gao, G. F.; Tatem, A. J.; Yu, H. Global epidemiology of avian influenza A H5N1 virus infection in humans, 1997-2015: a systematic review of individual case data. *Lancet Infect. Dis.* **2016**, *16*, e108−e118.
(54) Li, Q.; Zhou, L.; Zhou, M.; Chen, Z.; Li, F.; Wu, H.; Xiang, N.; Chen, E.; Tang, F.; Wang, D.; Meng, L.; Hong, Z.; Tu, W.; Cao, Y.; Li, L.; Ding, F.; Liu, B.; Wang, M.; Xie, R.; Gao, R.; Li, X.; Bai, T.; Zou, S.; He, J.; Hu, J.; Xu, Y.; Chai, C.; Wang, S.; Gao, Y.; Jin, L.; Zhang, Y.; Luo, H.; Yu, H.; He, J.; Li, Q.; Wang, X.; Gao, L.; Pang, X.; Liu, G.; Yan, Y.; Yuan, H.; Shu, Y.; Yang, W.; Wang, Y.; Wu, F.; Uyeki, T. M.; Feng, Z. Epidemiology of human infections with avian influenza A(H7N9) virus in China. *N. Engl. J. Med.* **2014**, *370*, 520−532.
(55) Frazee, B. W.; Rodriguez-Hoces de la Guardia, A.; Alter, H.; Chen, C. G.; Fuentes, E. L.; Holzer, A. K.; Lolas, M.; Mitra, D.; Vohra, J.; Dekker, C. L. Accuracy and Discomfort of Different Types of Intranasal Specimen Collection Methods for Molecular Influenza Testing in Emergency Department Patients. *Ann. Emerg. Med.* **2018**, *71*, 509−517 e1.
(56) Ruest, A.; Michaud, S.; Deslandes, S.; Frost, E. H. Comparison of the Directigen flu A+B test, the QuickVue influenza test, and clinical case definition to viral culture and reverse transcription-PCR for rapid diagnosis of influenza virus infection. *J. Clin. Microbiol.* **2003**, *41*, 3487−3493.
(57) McAuley, J. L.; Corcilius, L.; Tan, H. X.; Payne, R. J.; McGuckin, M. A.; Brown, L. E. The cell surface mucin MUC1 limits the severity of influenza A virus infection. *Mucosal Immunol.* **2017**, *10*, 1581−1593.
(58) Nakamura, S.; Horie, M.; Daidoji, T.; Honda, T.; Yasugi, M.; Kuno, A.; Komori, T.; Okuzaki, D.; Narimatsu, H.; Nakaya, T.; Tomonaga, K. Influenza A Virus-Induced Expression of a GalNAc Transferase, GALNT3, via MicroRNAs Is Required for Enhanced Viral Replication. *J. Virol.* **2016**, *90*, 1788−801.
(59) Nikitin, N.; Petrova, E.; Trifonova, E.; Karpova, O. Influenza virus aerosols in the air and their infectiousness. *Adv. Virol.* **2014**, *2014*, No. 859090.
(60) Alford, R. H.; Kasel, J. A.; Gerone, P. J.; Knight, V. Human influenza resulting from aerosol inhalation. *Proc. Soc. Exp. Biol. Med.* **1966**, *122*, 800−804.
(61) Zhu, X.; Viswanathan, K.; Raman, R.; Yu, W.; Sasisekharan, R.; Wilson, I. A. Structural Basis for a Switch in Receptor Binding Specificity of Two H5N1 Hemagglutinin Mutants. *Cell Rep.* **2015**, *13*, 1683−1691.

https://dx.doi.org/10.1021/acssensors.9b02126
ACS Sens. XXXX, XXX, XXX−XXX